Journal of Scientific Research & Reports

20(2): 1-17, 2018; Article no.JSRR.43311
ISSN: 2320-0227

Multi-model Analysis of the West African Monsoon: Seasonal Evolution and the Monsoon Onset

Alioune Badara Sarr[1], Moctar Camara[1*] and Ibrahima Diba[1]

[1]Laboratoire d'Océanographie des Sciences de l'Environnement et du Climat (LOSEC), Université Assane Seck de Ziguinchor, BP 523, Ziguinchor, Senegal.

Authors' contributions

This work was carried out in collaboration among all authors. Authors ABS and MC organised and wrote the paper. All authors discussed the results and contributed to the manuscript.

Article Information

DOI: 10.9734/JSRR/2018/43311
Editor(s):
(1) Dr. Rahul Kumar Jaiswal, National Institute of Hydrology, WALMI Campus, Bhopal, India.
(2) Dr. Mahmoud Nasr, Sanitary Engineering Department, Faculty of Engineering, Alexandria University, Egypt.
(3) Dr. Luigi Rodino, Professor of Mathematical Analysis, Dipartimento di Matematica, Università di Torino, Italy.
Reviewers:
(1) Zhiwei Zhu, Nanjing University of Information Science and Technology (NUIST), China.
(2) Gargi Akhoury, Birla Institute of Technology, India.
(3) Jun–Ichi Yano, Météo-France and CNRS, France.
Complete Peer review History: http://www.sciencedomain.org/review-history/26201

Original Research Article

Received 14 June 2018
Accepted 25 August 2018
Published 13 September 2018

ABSTRACT

The economy of West Africa and particularly in the Sahel region depends primarily on agriculture. Most of its agricultural productivity is achieved during the monsoon season (July-September) when the greatest amount of rain is recorded. The goal of this paper is to study the seasonal evolution of West African rainfall with a special focus on the onset of monsoon using five (5) regional climate models (RCMs) involved in the CORDEX (Coordinated Regional climate Downscaling Experiment) program. These RCMs have a horizontal resolution of 0.44° × 0.44° (about 50 km) and are initialised and forced to their lateral boundaries by the ERA-Interim reanalysis. The results show that the intra-seasonal variability of the West African monsoon (WAM) is well reproduced by RCMs despite the presence of some biases. The analysis of the dynamics of the West African monsoon shows that almost all models simulate a strong increase of the heat flux over the Sahara desert especially on its western part which promotes a substantial rise in the monsoon flow over the Sahel. This increase of low-level monsoon flow may induce an enhancement of the low-level specific humidity and the convective activity over the Sahel just after the onset. Moreover, the RCMs show a northward position and an intensification of the AEJ just

**Corresponding author: E-mail: moctar.camara@univ-zig.sn, moctar1sn@yahoo.fr;*

before the monsoon onset. The upper levels divergence seasonal evolution is similar with the rainfall band with collocation of the maxima suggesting that it may be used as a tool to better forecast the WAM onset.

Keywords: Regional climate models; onset; precipitation; seasonal evolution.

1. INTRODUCTION

The Sahel region is one of the most vulnerable regions to climate variability and climate change in West Africa [1,2]. Sahel is mostly covered by semi-arid regions known for their unreliable rainfall regime which is highly variable on intra-seasonal, inter-annual and interdecadal timescales [3,5]. Such variability influences the distribution and statistics of daily rainfall and extremes and can result in more frequent and severe drought and floods and delayed rainy season [6-8]. The Sahel economy depends heavily on agriculture. Most of its agricultural productivity is obtained during the rainy season (July-August-September), which corresponds to a strong convergence of the monsoon flow of south-southeast and a weak Harmattan of north-northeast. The southern displacement of the Inter-Tropical Convergence Zone (ITCZ) is characterised by a succession of phases of intensification and pauses of rainfall [9,10]. As rainfall is the primary source of water for various crops over the Sahel, this may substantially impact crop productivity and food security [11]. The ITCZ is located between mid-April and June at 5°N marking the rainy season in the Guinean zone. It then migrates towards 10°N between the end of June and September marking the rainy season in the Sudan-Sahel zone. This transition from the first maximum to the second maximum precipitation is called the monsoon onset [12,13]. The onset date corresponds to the installation phase of the monsoon over the Sahel band. The land-sea surface temperature difference between the continent (Sahel and Sahara) and the ocean (Gulf of Guinea) dominates the West African Monsoon (WAM) onset. The land-sea surface and temperature differences are also of great importance in the East Asia Subtropical Monsoon Onset [14,16]. The knowledge of the monsoon onset date has crucial importance for the crop yield and the management of water resources in the Sahel region. The sowing of the crop is largely connected with the start of the rainy season as pointed out by some previous studies [17,18].

Due to this, several studies have focused on the dynamics of the West African climate around this date. Among which Sultan and Janicot [12] performed such study with *in situ* data. Sijikumar et al. [19] and Diallo et al. [20] conducted similar study with regional climate models simulations. This work is based on the analysis of CORDEX regional climate models (RCMs). CORDEX is an international program implemented by several research centres, which aim at producing reliable climate change scenarios for impact and adaptation studies. The data from the ERA-Interim reanalysis of the European Center for Medium-Range Meteorological Forecasting (ECMWF) [21] covering the period 1989-2008 has been used to produce present day simulations that are intended to evaluate the performance of the CORDEX RCMs. For instance, some authors [22-24] have demonstrated that the CORDEX RCMs reproduce well with the rainfall and the temperature distribution during the WAM and that the mean ensemble average of all models generally outperforms the individual RCMs members. In the framework of CORDEX program, a series of experiments were also designed to obtain climate change projections that can be used for impact and adaptation studies. These simulations cover the period of 1951-2100 including the recent historical period, as well as the whole 21st century. The CORDEX program has been described in details by Giorgi et al. [25].

This study aims at analysing the seasonal evolution of WAM rainfall with a focus on the monsoon onset by using five (5) regional climate models of the CORDEX program during the period of 1989-2008.

Section 2 describes the data and methods used in this study. In section 3, the results are presented. The last part of this work is dedicated to the conclusion and outcomes.

2. DATA AND METHODS

2.1 Models Description and Experiment

RCMs are the area limited models which are used to dynamically disaggregate the global climate models (GCMs) [26]. They simulate the

climate at the regional scale. In this work, high resolution simulations were used (0.44°×0.44°, approx. 50 km) resulting from 5 RCMs of the CORDEX-Africa program: CCLM4, RCA4, RACMO22T, CanRCM4 and HIRHAM5. These models are forced by the ERA-Interim reanalysis which is the third generation of the European Centre for Medium-range Weather Forecasting (ECMWF) data reanalysis. The simulations are integrated over the whole Africa domain from 1989 to 2008. The model's institutions and the references are shown in Table 1. The study area considered in this work (Fig. 1) exhibits some highlands localised around Cameroon (Cameroon mountains, CM), Central Nigeria (Jos plateau, JP) and the Republic of Guinea (Guinea highlands, GH).

2.2 Observation Data

The validation data for rainfall come from the Global Precipitation Climatology Project (GPCP; [27,28]). Previous studies [22,7] have reported that the GPCP climatology represented well the spatial and temporal distribution of West african rainfall. These data as well as the Era-interim reanalysis are described in Table 2.

2.3 West African Monsoon Index (WAMOI)

To study the dynamics of the West African climate around the onset date, the West African Monsoon Index (WAMOI) was computed [19]. The Guinea (10°W-10°E; 0°-7.5°N) and the Sahel (10°W-10°E; 7.5N-20°N) rainfall indexes have been calculated using the mean rainfall for 5-days (or pentad) in the first step. The standardised difference between the Sahel rainfall index (SI) and Guinea rainfall index (GI) are calculated afterwards. If the difference (SI-GI) is positive (negative) then the Sahelian rainfall rate is higher (lower) than Guinean rainfall rate. The mean onset date corresponds to the first pentad just above the 0 threshold for at least three successive pentads.

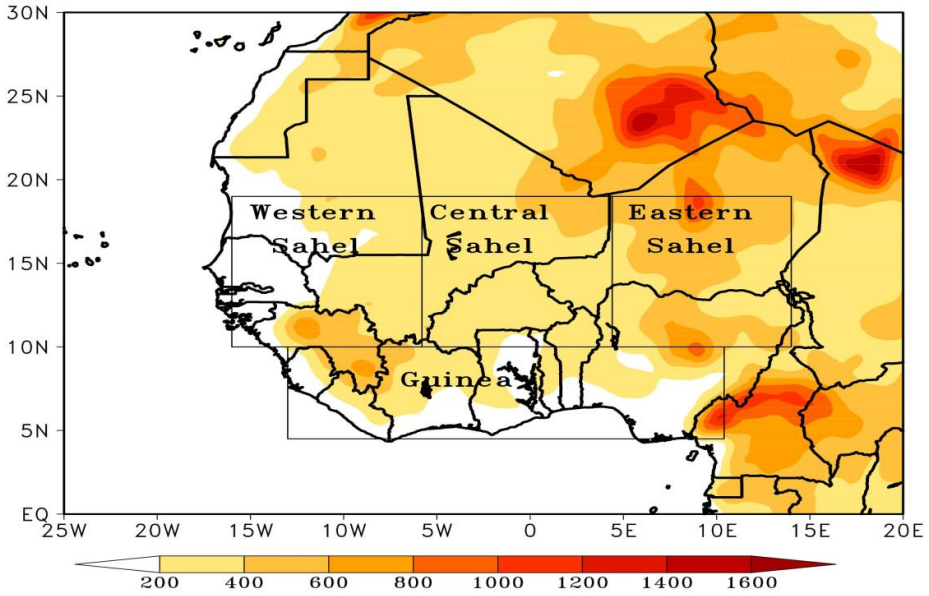

Fig. 1. Topography of the study domain (West Africa) and considered sub-domains (Western Sahel, Central Sahel, Eastern Sahel and Guinea)

Table 1. Description of the regional climate models

Name	Institution	References
CCLM4	CLM-community	Baldauf et al. [29]
RACMO22T	KNMI, The Netherlands	Van Meijgaard et al. [30]
RCA4	SMHI, Sweden	Samuelsson et al. [31]
CanRCM4	CCCma, Canada	Scinocca et al. [32]
HIRHAM5	DMI, Denmark	Christensen et al. [33]

Table 2. Description of the validation data and Era-interim reanalysis

	GPCPV22	ERA-interim
Spatial resolution	2.5° in monthly 1° in daily	0.75°
Spatial coverage	Land and Ocean	Land and ocean
Temporal coverage	Monthly :1979-2015 Daily : 1997-2015	Monthly and daily : 1979-to present
References	Adler et al. [27]; Huffman et al. [28]	Dee et al. [34]

3. RESULTS

3.1 Validation of the Mean Summer Rainfall

The distribution of the summer rainfall (July-September) over West Africa is presented in Fig. 2; while Table 3 summarises the mean bias (MB), the root mean square error (RMSE) and the pattern correlation coefficient (PCC) for the models and the ERA-Interim reanalysis with respect to GPCP observations. The RMSE measures the amplitude of errors committed by models; while the mean bias characterises the sign of errors (overestimation or underestimation). The PCC allows to characterise the linear interdependence of two climate parameters.

GPCP Climatology exhibits a north-south rainfall gradient with a maximum localised over the orographic areas (Fouta Djallon Mountain, Cameroon Mountains, Jos Plateau). Almost all RCMs have shown a dry bias over the western Sahel except HIRHAM5 model (Fig. 2g). This model strongly overestimates the rainfall intensity mostly over the entire West Africa (up to 27%) except Western Sahel and more particularly over the Senegal where a dry bias is present [21]. The strongest dry bias is shown by CCLM4 model (Fig. 2f) (about 50%) over Western Sahel. The RMSE over this region is generally weak for the RCMs with a good PCC (up to 0.6) except for HIRHAM5 model (about 0.4). In Central and Eastern Sahel, almost all RCMs have recorded wet biases except RCA4 which exhibits a dry bias on the most part of the study region (about 12%).

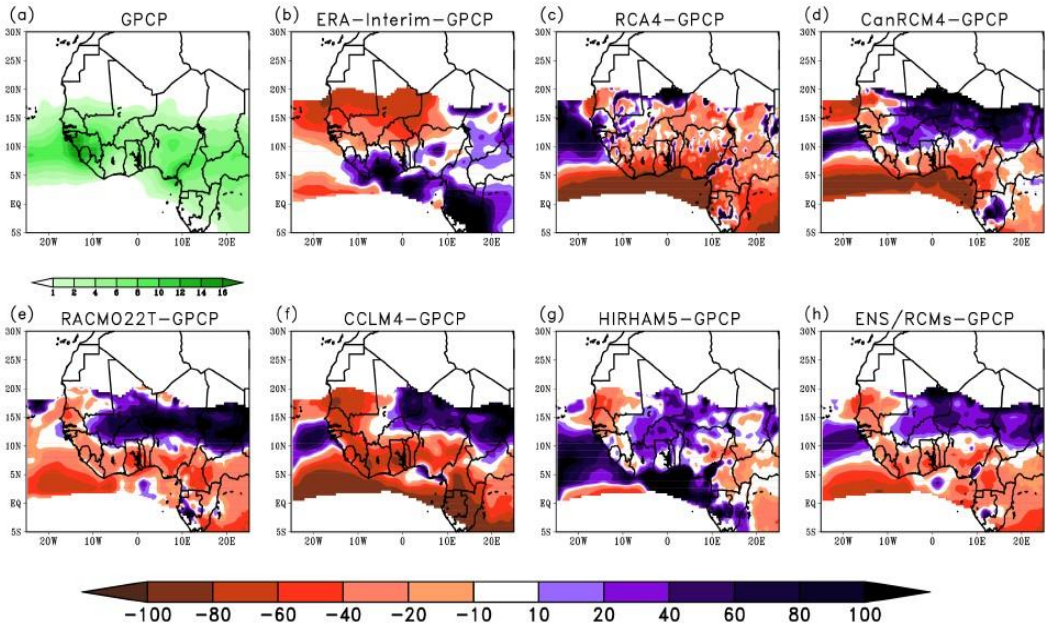

Fig. 2. Mean JAS rainfall (mm/day) averaged from 1989 to 2008 for: a. GPCP and the biases with respect to GPCP (expressed in %) for b. ERA-Interim, c. RCA4, d. CanRCM4, e. RACMO22T, f. CCLM4, g. HIRHAM5 and h. ensemble mean of all models

Table 3. Mean bias (MB) expressed in %, root mean square error (RMSE) expressed in mm/day and pattern correlation coefficient (PCC) of the mean summer (JAS) rainfall for the RCMs and ERA-interim reanalysis with respect to GPCP observation

Model	Western Sahel		Central Sahel		Eastern Sahel		Guinea		West Africa		
	Mean bias	RMSE	Mean bias	RMSE	Mean bias	RMSE	Mean bias	RMSE	Mean bias	RMSE	PCC
CCLM4	-50	3.4	1.6	2.1	1.9	2.1	-47.9	4.1	-19.6	3.4	0.6
RACMO22T	-2.1	3	42.9	3.9	31.6	3.3	-32.2	3	0.5	2.8	0.6
RCA4	-5.7	2.5	-23.6	1.1	-30	1	-38.9	4.6	-12.4	2.9	0.7
CanRCM4	-4.2	2.5	22.7	2.4	16.2	2.2	-34.6	3.2	-2.6	2.4	0.8
HIRHAM5	6.8	3.3	45	3.9	21.4	2.9	28.1	6.3	27	4.2	0.4
ENS/RCMs	-10.7	1.8	17.9	2.1	8.5	1.8	-25.1	2.9	-1.9	2.1	0.8
ERA-Interim	- 40	6.4	-54.5	2.4	-24.5	2.4	13.8	2.4	-7.6	2.2	0.6

This large underestimation simulated by this model is in line with the findings of Dee et al. [34]. The strongest wet bias is simulated by the HIRHAM5 (Fig. 2g) and RACMO22T models (Fig. 2e) (about 45% and 42%, respectively) over Central Sahel. These biases have been found to be very weak for the CCLM4 model in Central and Eastern Sahel (about 1.6% and 2%, respectively). In Guinea zone, only the HIRHAM5 model displays a wet bias (up to 28%). The other RCMs show dry biases in this area. The strongest dry bias (up to 47%) is exhibited by the CCLM4 model followed by RCA4 and CanRCM4 models in this region. This latter model exhibits a good PCC over the study area (about 0.8). When considering the RMSE, it is stronger in the Guinea region compared to the Sahel area. The ensemble mean of models has exhibited the weakest biases (below 2%) and a good PCC (exceeding 0.8) over the study region. Thus, the ensemble mean of all models outperforms the individual RCMs members in coherence with some previous works [22,23,35,36]. The forcing data (ERA-Interim) records an important dry bias in most of the Sahel region and a weak wet bias (<14%) along the Guinean zone. This configuration seems to be in opposition (except the Western Sahel) with that of CCLM4, CanRCM4 and RACMO22T simulations and the ensemble mean of the models (Fig. 2h). These reveal a dry bias over Guinea and a positive rainfall bias over most part of the Sahel. Thus, biases of the RCMs do not depend only on the forcing data because internal variability of models may play a strong role too [37].

3.2 Intraseasonal Variability of the West African Monsoon

In order to better understand the latitudinal progression of the WAM, the hövmoller diagram of 5-day mean precipitation (or pentad) averaged between 10°W and 10°E for GPCP observation, ERA-Interim reanalysis, the RCMs and their ensemble mean are displayed in Fig. 3. The mean onset date is also indicated in the figure by the vertical line.

The GPCP climatology has exhibited three phases: the first phase corresponds to a rainfall centred maximum around 5°N until the second half of June. This is the beginning of the first rainy season in the Guinean zone. A strong reduction of the rainfall has been noted followed by an increase towards 10°N signifying the start of the rainy season in the Sahelian zone by the end of June (second phase). Finally, the GPCP climatology exhibits a progressive southward retreat of the rain band between September and October (third phase) corresponding to the second rainy season in the Guinean zone.

The ERA-Interim reanalysis (Fig. 3b) reproduces quite well with these three phases but some differences appeared. Indeed, the first rainfall peak intensity is underestimated while the second rainfall maximum is overestimated. The ERA-Interim reanalysis also shows a monsoon jump at later stage.

Clearly the RCMs simulate the northward shift of the ITCZ to the Sahel region. However, the CCLM4 and HIRHAM5 models (Fig. 3f and 4g respectively) overestimate the magnitude of the first rainfall peak (between 2°S and 6°N); which is in coherence with Nikulin et al. [22]. The magnitude of the second peak has been underestimated in the CCLM4 model. It should also be noted that HIRHAM5 model tends to simulate the monsoon jump too late (second half of July). As for RCA4 model (Fig. 3c), it presents a strong underestimation of the rain band and fails to quite reproduce the monsoon jump, and this is consistent with the findings of Akinsanola et al. [38]. The RACMO22T model (Fig. 3e) underestimates the magnitude of the first rainfall peak. The second peak rainfall of this model is too wide compared to other observations. Considering the CanRCM4 model (Fig. 3d), the observed rainfall peaks are in general well reproduced. The ensemble mean of the RCMs also records the monsoon jump rather well with the first rain band more intensely and more extensively compared to that of GPCP observations.

The main driving forces of the ITCZ propagation northward to the Sahel are the low-level meridional flow (between surface and 800hPa), the AEJ (between 500-700hPa) associated with the intense solar heating over the Sahara [12,39,40,20].

Fig. 4 presents the hövmoller diagram of 5-day mean of wind divergence at 850 hPa from the ERA-Interim reanalysis, the RCMs and their ensemble mean average along 10°W-10°E. Negative (positive) values refer to convergence (divergence) respectively. The ERA-Interim data (Fig. 4a) displays a weak convergence over the Guinea region (near 2°N) during the beginning of April until the end of May which has shifted northward to the Sahel (near 10°N) before the onset date until the southward retreat.

Compared to the reanalysis, these models have a relatively similar structure with different magnitudes. RCA4, CanRCM4 models and the ensemble mean of RCMs (Fig. 4b, 4c and 4g, respectively) underestimate the first convergence peak over the Guinean zone. RACMO22T, CCLM4 and HIRHAM5 models (Fig. 4d, 4e and 4f respectively) show rather well the first peak convergence in the Guinean zone with a displacement towards the north (10°N) over the Sahelian zone before and after the onset date. These three models simulate a convergence band much broader and more intense than the reanalysis data over the Sahelian zone. This is in agreement with the rainfall patterns.

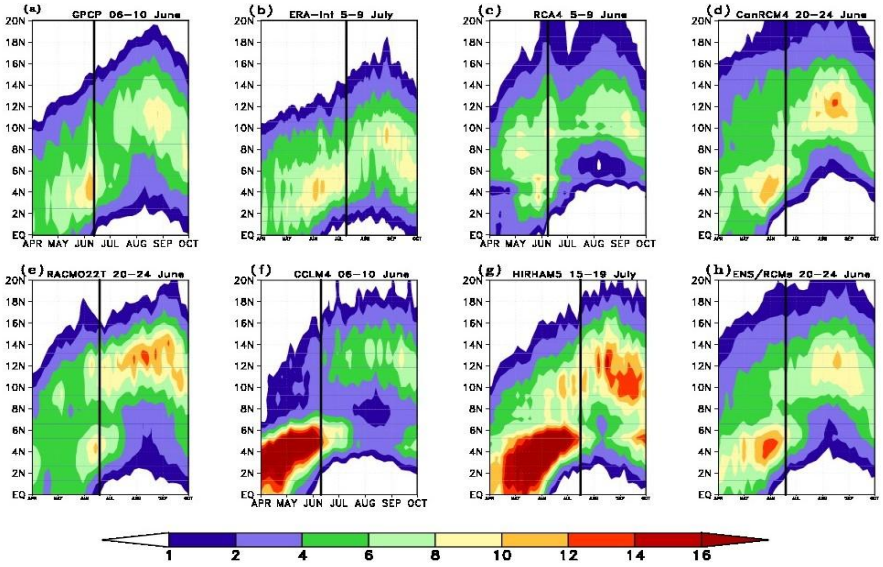

Fig. 3. Time/latitude diagram of the 5-day mean of precipitation (mm/day) averaged from 1989 to 2008 for: a. GPCP b. ERA-Interim, c. CCLM4, d. RCA4, e. RACMO22T f. CanRCM4, g. HIRHAM5 and h. ensemble mean of all models. The mean onset date is indicated by the vertical line

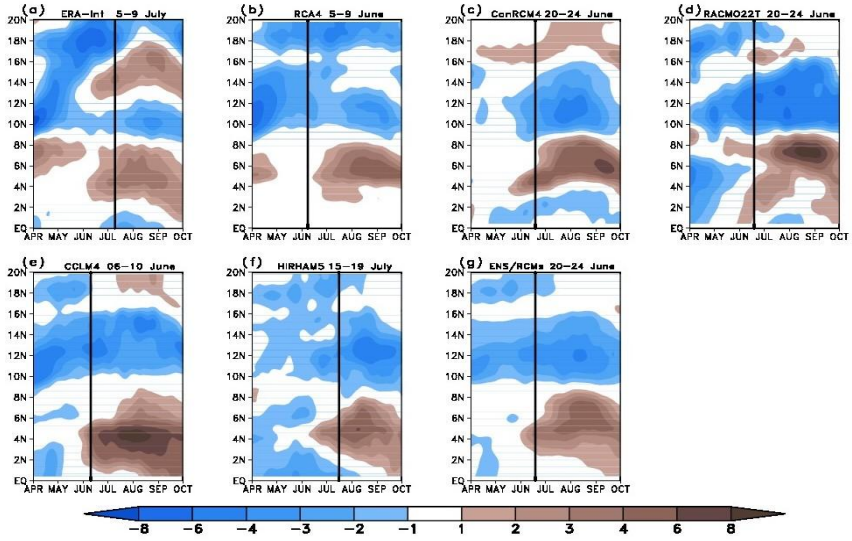

Fig. 4. Time/latitude diagram of the 5-day mean of wind divergence at 850 hPa (multiplied by 106s-1) during the period 1989-2008 for : a. ERA-Interim, b. RCA4, c. CanRCM4, d. RACMO22T, e. CCLM4, f. HIRHAM5, g. ensemble mean of all models. The mean onset date is indicated by the vertical line

The hövmoller diagram of 5-day mean wind divergence at upper levels (200hPa) averaged along 10°W-10°E is represented in Fig. 5. An upper-level divergence situation is known to promote deep convection.

The ERA-Interim reanalysis (Fig. 5a) shows a maximum of wind divergence over the Guinean zone between April and May followed by a second one just after the onset over the Sahel.

This distribution is well reproduced by all RCMs and their ensemble mean except RACMO22T. The latter model does not simulate the guinea peak and it strongly overestimates the Sahel maximum, resulting in an overestimation of Sahel rainfall (Fig. 3). The ensemble mean of all models displays a seasonal evolution similar to that of the rainfall with a colocation of the Guinean and Sahelian peaks. This result suggests that the upper-level divergence may be a good indicator in the forecasting of the onset of monsoon in the Sahel region.

The 5-day mean relative vorticity at 500 hPa average along 10°W-10°E is depicted in Fig. 6. When the relative vorticity is positive (negative), this situation corresponds to a cyclonic circulation (anticyclonic circulation).

The ERA-Interim reanalysis shows a cyclonic circulation over the rain band with a maximum localised between the latitudes 6°N and 12°N from the beginning of June until the monsoon retreat phase with a minimum cyclonic circulation over the Guinea area.

The RCA4 model (Fig. 6b) fails to accurately reproduce this distribution. This model simulates an anticyclonic circulation over the rain band area and a cyclonic circulation below this band. That is consistent with the strong underestimation of the rainfall peaks simulated by this model. The other models reproduced rather well the patterns of the ERA-Interim reanalysis. Nevertheless, they exhibit a slight differences. The circulation is slightly overestimated in the CanRCM4, RACMO22T models and the ensemble mean of the models (Fig. 6c, 6d and 6g respectively) which show a strong cyclonic circulation just after the onset over the Sahel region. CCLM4 and HIRHAM5 models (Fig. 6e and 6f, respectively) simulated a cyclonic circulation much more intense and more extensive over Guinea (between 2°N and 6°N) than the ERA-Interim reanalysis. In the southern Sahel (between 10°N-12°N), CCLM4 underestimates this circulation while HIRHAM5 model overestimates it.

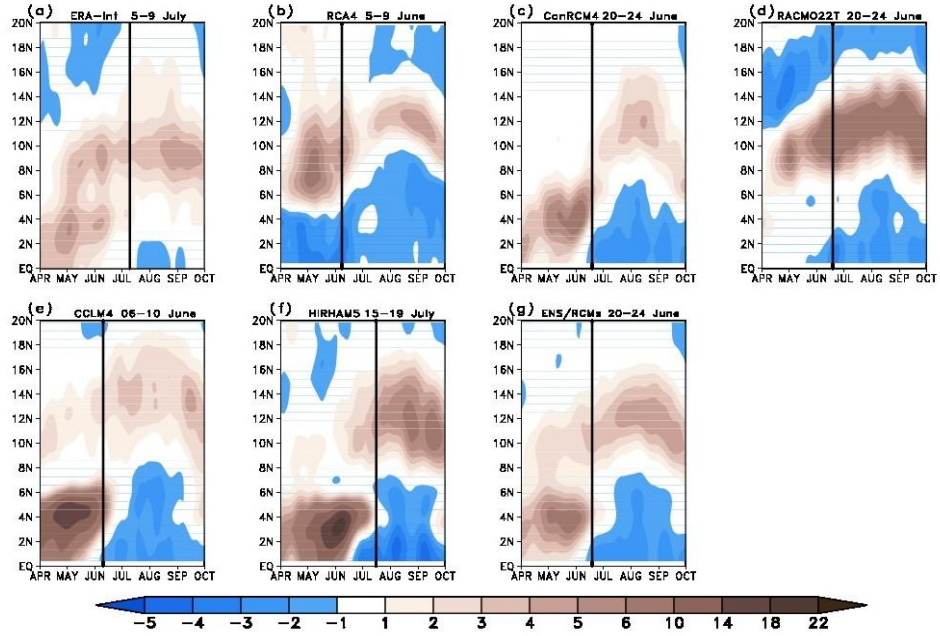

Fig. 5. Time/latitude diagram of the 5-day mean of wind divergence at 200 hPa (multiplied by 106s-1) during the period of 1989-2008 for: a. ERA-Interim, b. RCA4, c. CanRCM4, d. RACMO22T, e. CCLM4, f. HIRHAM5, g. ensemble mean of all models. The mean onset date is indicated by the vertical line

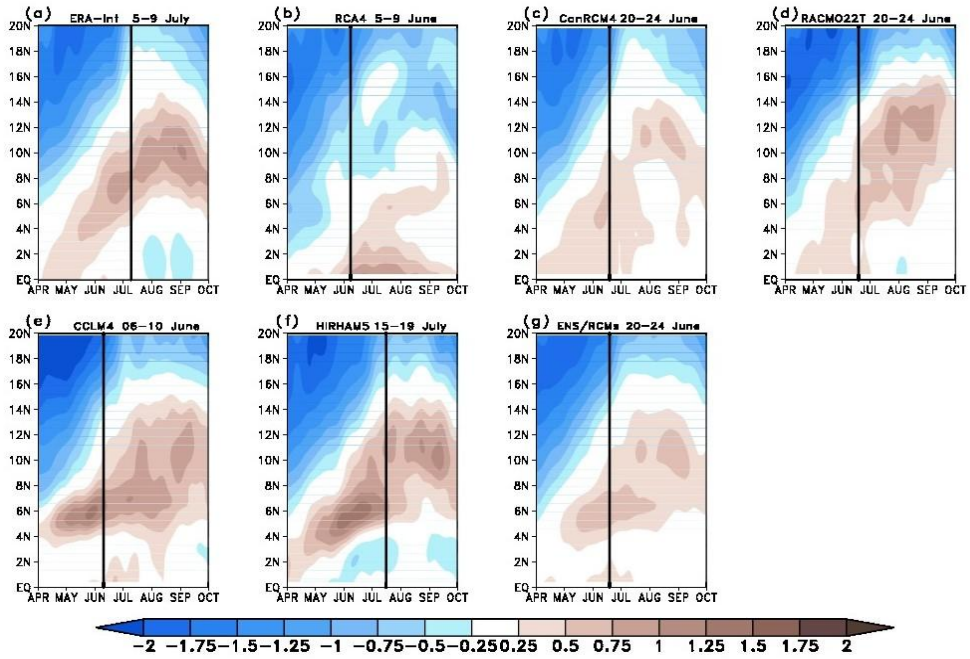

Fig. 6. Time/latitude diagram of the 5-day mean of relative vorticity at 500 hPa (multiplied by 105s-1) averaged from 1989 to 2008 for : a. ERA-Interim, b. RCA4, c. CanRCM4, d. RACMO22T, e. CCLM4, f. HIRHAM5, g. ensemble mean of all models. The mean onset date is indicated by the vertical line

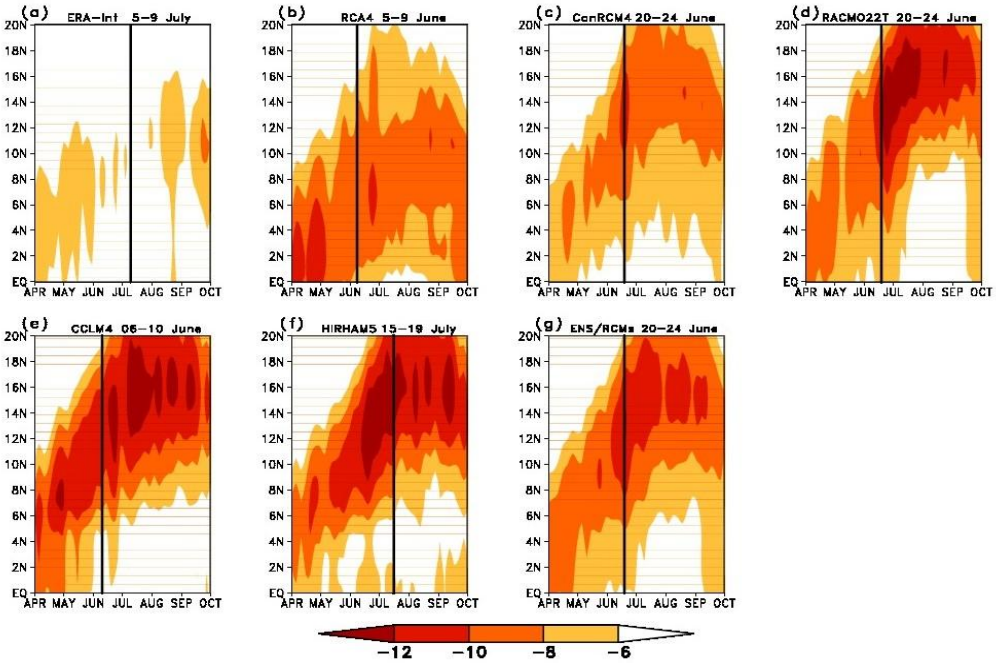

Fig. 7. Time/latitude diagram of the 5-day mean of zonal wind at 500 hPa averaged from 1989 to 2008 for:a. ERA-Interim, b. RCA4, c. CanRCM4, d. RACMO22T, e. CCLM4, f. HIRHAM5, g. ensemble mean of all models. The mean onset date is indicated by the vertical line

Figs. 7 and 8 show respectively the seasonal distribution of the 5-day mean zonal wind at 500hPa and 200hPa from ERA-Interim reanalysis, the RCMs and their ensemble mean. These two levels are used to focus on the analysis of the characteristics of the mid-levels African Easterly Jet (AEJ) and the upper levels Tropical Easterly Jet (TEJ). The AEJ appears over West Africa during the boreal summer as the result of the strong meridional surface moisture and temperature gradients between the Sahara and equatorial Africa. It is located around 15°N [41-43]. The TEJ is associated with the upper-level outflow from the Asian monsoon. It is centered on 10°N. An AEJ position more northward associated with a strong TEJ is favourable to the rainfall reinforcement over the Sahel region [44].

The ERA-Interim data at 500hPa (Fig. 7a) exhibits a maximum of zonal wind between April and June over the Guinean region followed by another maximum in the Sahel region in August-September period. The AEJ seasonal evolution is well captured by the RCMs and their ensemble mean. However, there are some differences. In fact, all simulations tend to strongly overestimate the strength of the mid-levels easterly flow. Moreover, the AEJ is located more northward when considering the models and their ensemble mean except the RCA4 model. Moreover, CCLM4 and RACMO22T models exhibit a reinforcement of the AEJ intensity just before the onset.

When the zonal wind at 200hPa is considered, the ERA-Interim reanalysis (Fig. 8a) shows a reinforcement of the TEJ after the WAM onset. All simulations reproduce this distribution but the strength of the easterly flow core is largely overestimated by the RCMs. The RCA4 model (Fig. 8b) tends to locate the TEJ core more northward. This analysis suggests that the TEJ may not play a key role in the establishment of the monsoon (onset) over West Africa.

3.3 West African Monsoon Onset

This part of the study is about the dynamics of the WAM during the onset period. When detecting the mean onset date following [19] (Fig. 9), In the present study it has been found that it is located in the 33rd pentad (11-15 June) for GPCP which is in line with Sijikumar et al. [19]. The RCA4 and CCLM4 models have simulated the mean onset date very earlier. It has been observed that in the 30th pentad (01-05 June) and in the 31st pentad (06-10 June), respectively. CanRCM4, RACMO22T models and the ensemble mean of RCMs capture the mean onset later (35th pentad or 21-25 June). This date is very close to that

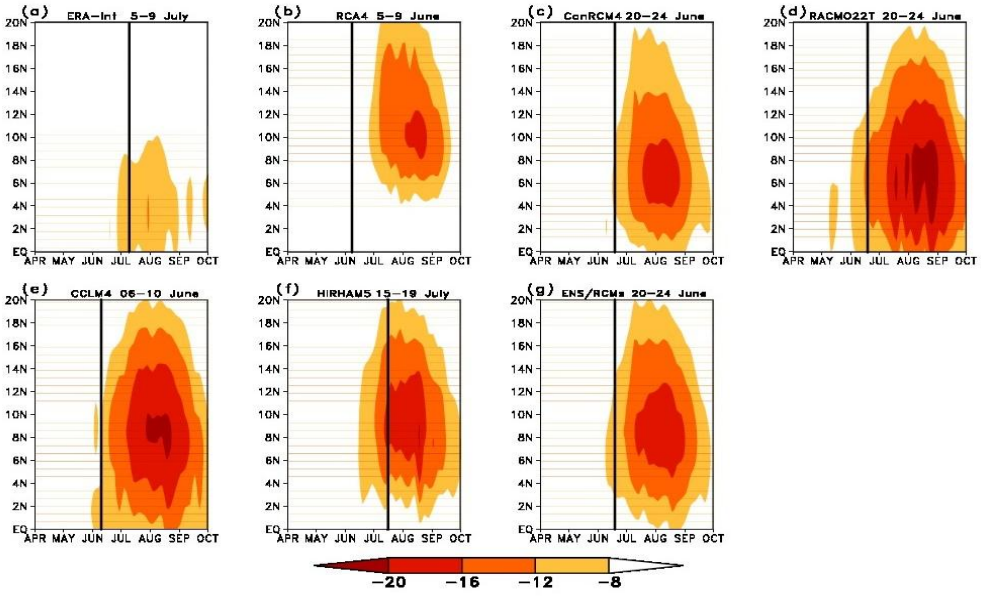

Fig. 8. Time/latitude diagram of the 5-day mean of zonal wind at 200 hPa averaged from 1989 to 2008 for : a. ERA-Interim, b. RCA4, c. CanRCM4, d. RACMO22T, e. CCLM4, f. HIRHAM5, g. ensemble mean of all models. The mean onset date is indicated by the vertical line

was found by Sultan and Janicot [12], i.e., June 24th. Diaconescu et al. [45] using the CanRCM4 model also found the mean onset in the same pentad, i.e., 35th pentad. The HIRHAM5 model and ERA-Interim reanalysis show very late monsoon jump; their mean onset dates are located in the 39th pentad (11-15 July) and the 37th pentad (01-05 July), respectively. These two previous onset dates are far from the GPCP climatology date.

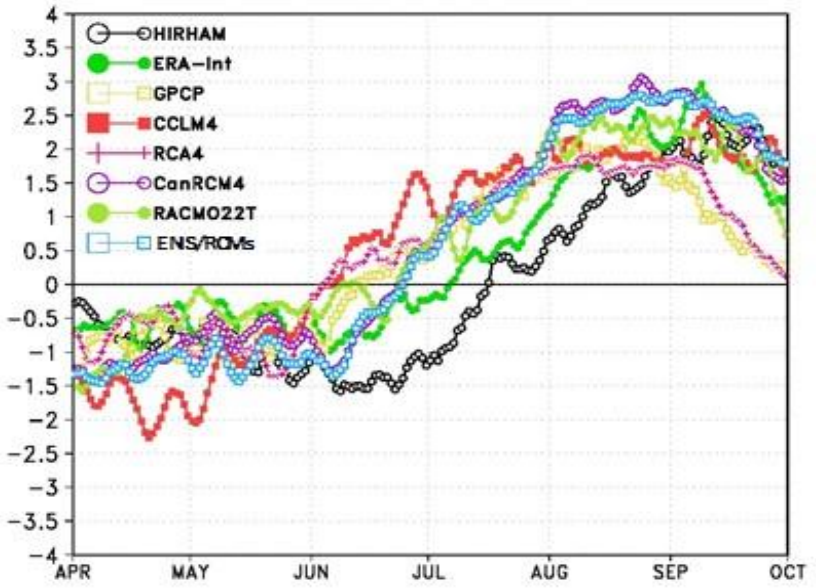

Fig. 9. Standardised differences between the Sudan-Sahel rainfall index (10°W-10°E, 7.5°N-20°N) and the Guinea rainfall index (10°W-10°E, 0°-7.5°N) for: GPCP, ERA-Interim, RCA4 , CanRCM4, RACMO22T, CCLM4, HIRHAM5 and the ensemble mean of all models during the period 1997 to 2008

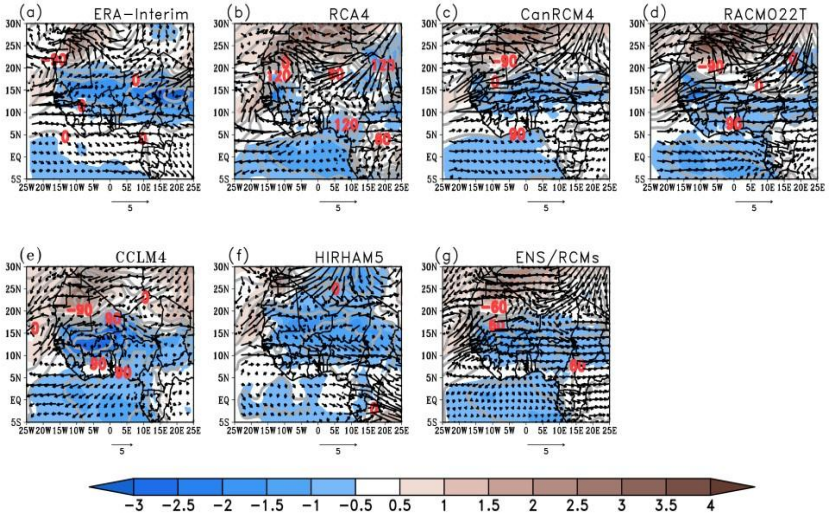

Fig. 10. The composite difference of 3 pentads after onset and 3 pentads before onset (after minus before) of 850 hPa wind (arrows in m/s) superimposed over the 2 m air temperature (shading in °C) and the mean sea level pressure (contour in hPa) for: a. ERA-Interim, b. RCA4, c. CanRCM4, d. RACMO22T, e. CCLM4, f. HIRHAM5 and g. ensemble mean of all models during the period of 1997 to 2008

After the detection of the onset dates, three (3) successive pentads located before and after the onset date for the composite study are shown below.

The mean difference (after onset minus before onset) of the low-level (850 hPa) wind superimposed over the 2 m air temperature and the mean sea level pressure is displayed in Fig. 10.

ERA-Interim reanalysis (Fig. 10a) shows an increase of the westerly flow from the Atlantic Ocean to the Sahel band (10°N-12°N). This increase is driven by the north-south pressure gradient due to the intense heat low in Western Sahara (or Saharan heat low). The Saharan heat low plays a significant role in the monsoon jump process [40,46]. Therefore, the bias in onset date could be partly explained by the Saharan heat low dynamics [12].

The meridional temperature gradient is realistically simulated by the RCMs and the ensemble mean of all models which display the same spatial pattern obtained with the reanalysis data except the HIRHAM5 model. This may explain the origin of the important anomaly in the onset date simulated by the HIRMHAM5 model (Fig. 10f). Furthermore, the magnitude of the Saharan heat low in the CanRCM4, RACMO22T, CCLM4 models (Fig. 10c, 10d and 10e, respectively) and their ensemble mean (Fig. 10g) is greater than that of the ERA-interim reanalysis.

This intensifying heat low could be at the origin of the strong north-south pressure gradient. According to Sijikumar et al. [19], this gradient forces the moist air of the ocean to penetrate inside the continent and leads the meridional component of the wind across Guinea in the Sudan-Sahel region. This may explain the wet rainfall biases simulated by these models in large parts of the Sahel region.

Fig. 11 shows the mean difference (after minus before onset) of the low-level (850 hPa) specific humidity from the ERA-Interim reanalysis, the RCMs and their ensemble mean.

The ERA-Interim reanalysis has a dipolar structure clearly showing an increase of the low-level specific humidity over the Sahel and the Sahara and a reduction over the Guinean area just after the onset. CanRCM4, RACMO22T models (respectively Fig. 11c and 11d) and the ensemble mean of the models (Fig. 11g) show an increase in a narrow band over the Central

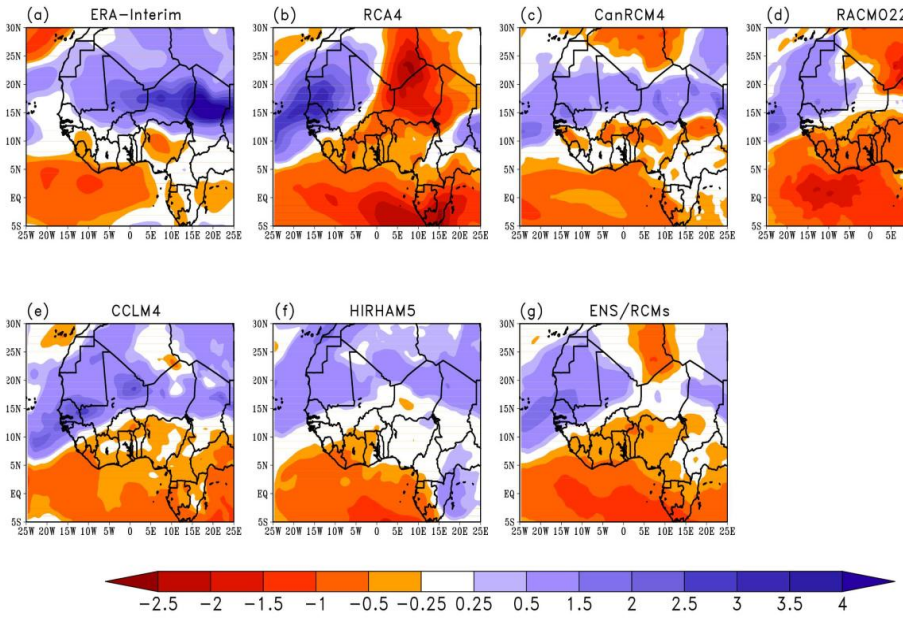

Fig. 11. The composite difference of 3 pentads after onset and 3 pentads before onset (after minus before) of specific humidity at 850 hPa (g/kg) for: a. ERA-Interim, b. RCA4 , c. CanRCM4, d. RACMO22T, e. CCLM4, f. HIRHAM5 and g. ensemble mean of all models during the period 1997 to 2008

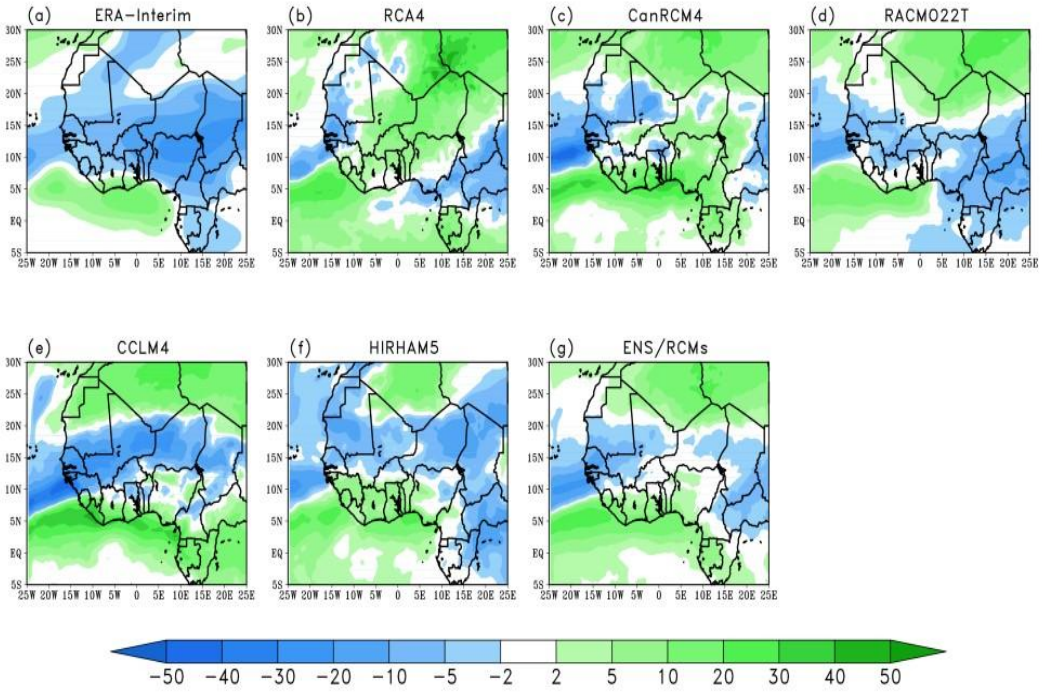

Fig. 12. The composite difference of 3 pentads after onset and 3 pentads before onset (after minus before) of the outgoing longwave radiation (W.m-2) for: a. ERA-Interim, b. RCA4, c. CanRCM4, d. RACMO22T, e. CCLM4, f. HIRHAM5 and g. ensemble mean of all models during the period 1997 to 2008

and East Sahel (between 14°N and 18°N). The HIRHAM5 model reveals clearly a dipole in West Africa when considering the low-levels specific humidity with an increase over the entire Sahel zone and a decrease over the whole Guinea area. The strong increase of the low-specific humidity over the Sahel zone is well correlated with the wet rainfall biases simulated by the RCMs over that region. Concerning the RCA4 model, it shows a slight humidity increase only over the Western Sahel which is in line with dry rainfall biases simulated by this model.

The mean difference (after minus before onset) of the outgoing long wave radiation (OLR) is represented on Fig. 12. The negative values (positive) correspond to an increase (reduction) in the convection. The ERA-Interim reanalysis (Fig. 12a) shows a strengthening of the convection over West Africa despite the presence of dry rainfall biases over the Sahel. The increase in the convective activity just after the onset over the Guinea area is consistent with the wet bias found in this area. RCA4 model (Fig. 12b) displays an increase in the convection over the western Sahel and particularly over the Senegal and Mauritania and a reduction over the rest of the study region. Regarding the CanRCM4 model, an increase over the Western Sahel and the North of the Central Sahel has been observed. A strong reinforcement of the convection over the Sahel is simulated by RACMO22T, CCLM4, HIRHAM5 models (Fig. 12d, 12e and 12f respectively) and by the ensemble mean of the models (Fig. 12g). This increase in the convection simulated by these models is also associated with wet rainfall biases over this region. Thus the increase in the convection just after the onset has also a positive impact on the installation of monsoon in the Sahel.

4. CONCLUSION

In this work, high resolution simulations (0.44° × 0.44°) performed by five (5) RCMs of CORDEX program which are forced over the period 1989-2008 by the ERA-Interim reanalysis, are analysed. Simulations resulting from these models and their ensemble mean are validated with GPCP climatology precipitation data and the Era-interim reanalysis data.

The analysis of the various results reveals that spatial distribution of West African rainfall is well reproduced by the RCMs. However, they exhibit certain differences. CanRCM4, CCLM4 and RACMO22T models present wet biases over the Central Sahel and the Eastern Sahel and dry biases over the rest of the domain. As for the model HIRHAM5, it displays wet biases over a large part of West Africa; while the RCA4 model shows a dry bias over the whole domain. These biases are generally weak in the RCMs ensemble in coherence with previous findings [22].

The main characteristics of the intra-seasonal variability of rainfall (monsoon onset and the installation and retreat phases) have been studied. They are generally well reproduced by the models and their ensemble mean. Some differences between the RCMs and GPCP observations on the positioning, duration and intensity of the rainfall peak are also noted but the monsoon jump was clearly captured by these models with certain differences; it appeared earlier in RCA4 and CCLM4 models and later in other models and the multi-model ensemble.

The analysis of the hövmoller diagram of 5-day mean winddivergence at upper levels (200hPa) exhibits a seasonal evolution similar to that of the rainfall with a colocation of the Guinean and Sahelian peaks. This result suggests that the upper-level divergence may be a good indicator for the forecast of the onset date in the Sahel region.

Concerning the zonal wind at 500hPa and 200hPa, the RCMs exhibits a reinforcement of the AEJ and located it more northward before and after the WAM onset compared to the ERA-Interim reanalysis except for the RCA4 model. Furthermore, an intensification of TEJ has been diagnosed just after the West African monsoon onset.

The analysis of some key parameters involved in the monsoon onset shows that the ERA-Interim reanalysis and RCMs simulate an increase of the specific humidity at 850 hPa just after the onset over the Sahel and the Sahara except for RCA4 which presented a reduction on the Central Sahel the Eastern Sahel. RACMO22T and CanRCM4 also show a reduction over the North of the Central Sahel, the Eastern Sahel and over the Sahara.

When considering the composite difference of the meridional gradient of temperature, ERA-Interim presents a slight increase over the Sahara especially on its Western part and a reduction over the Sahel and the Guinean zone. This structure creates a pressure gradient between the continent and the equatorial Atlantic Ocean which is at the origin of the westerly monsoon flow. All models except RCA4 overestimated this meridional gradient which translated into a stronger moisture flux compared to ERA-Interim reanalysis.

Despite the presence of some biases, this work reveals the ability of the MCRs to represent well the West African climate and to understand the key processes involved in the onset of the WAM. It needs to be continued by analysing the CORDEX climate change projections to determine the behaviour of the West African monsoon during the near and the far future.

ACKNOWLEDGEMENTS

The authors would like to thank the Assane SECK University and the project "Fonds d'Impulsion de la Recherche Scientifique et Technique (FIRST)" for their support.

COMPETING INTERESTS

Authors have declared that no competing interests exist.

REFERENCES

1. Nicholson SE, Some B, Kone B. An analysis on recent rainfall conditions in West Africa, including the rainy season of 1997 ENSO year. J Clim. 2000;1:2628–2640.
2. Biasutti M, Giannini A. Robust Sahel drying in response to late 20th century forcings. Geophysics Research Letters. 11:L11706; 2006.
DOI: 101029/2006GL026067
3. Wang G, Eltahir EAB. Role of vegetation dynamics in enhancing the low-frequency variability of the Sahel rainfall. Water Resources Research. 2000;36.
DOI: 10.1029/1999WR900361
(ISSN NO: 0043-1397)
4. Jenkins GS, Gaye AT, Sylla MB. Late 20th century attribution of drying trends in the Sahel from the regional climate model (RegCM3). Geophysical Research Letters. 2005;32:L22705.
5. Hoerling M, Hurell J, Eischeid J, Phillips A. Detection and attribution of twentieth-

century northern and southern African rainfall change. The National Center for Atmospheric Research is Sponsored by the National Science Foundation; 2006.

6. Sylla MB, Giorgi F, Coppola E, Mariotti L. Uncertainties in daily rainfall over Africa: Assessment of observation products and evaluation of a regional climate model simulation. International Journal of Climatology; 2012.
DOI: 10.1002/joc.3551
7. Sylla MB, Dell'Aquila, Ruti PM, Giorgi FC. West African monsoon in state-of-the-science regional climate models. International Journal of Climatology; 2013. Available:www.wileyonlinelibrary.com
DOI: 10.1002/joc.2029
8. Diallo I, Sylla MB, Giorgi F, Gaye AT, Camara M. Multi-model GCM-RCM ensemble based projections of temperature and precipitation over West Africa for the early 21st century. International Journal of Geophysics. 2012; 972896:19.
DOI: 10.1155/2012/972896
9. Janicot S, Caniaux G, Chauvin F, de Coëtlogon G, Fontaine B, Hall N, et al. Intra- seasonal variability of the West African monsoon. Atmospheric Sciences Letters; 2010.
DOI: 10.1002/asl.280
10. Salack S, Sultan B, Oettli P, Muller B, Gaye AT, Hourdin F. Représentation de la pluie dans les modèles climatiques régionaux et application à l'estimation des rendements en mil. Sécheresse. 2012b; 23(1).
11. Traoré S, Agali A, Muller B, Kouressy M, Somé L, Sultan B, Oettli P, SiénéLaopé AC, Vintrou E, Sangaré S, Vaksmann M, Diop Mb, Bégué A, Dinghun M, Baron C. Characterizing and modelling the diversity of cropping situations under climatic constraints in West Africa. Atmospheric Science Letters; 2010.
DOI: 10.1002/qj.728
12. Sultan B, Janicot S. The West African monsoon dynamics. Part II: The "pre-onset" and "onset" of the summer monsoon. Journal of Climate. 2003;16: 3407–3427.
13. Fontaine B, Louvet S. Sudan-Sahel rainfall onset: Definition of an objective index, types of years, and experimental hindcasts. J. Geophys. Res. 2006;111: D20103.
DOI: 10.1029/2005JD007019
14. Zhu Z, Li T. Empirical prediction of the onset dates of South China Sea summer monsoon. Clim. Dyn. 2017;48(5):1633-1645.
15. Zhu Z, He J, Qi L. Seasonal transition of East Asian subtropical monsoon and its possible mechanism. J. Trop. Meteor. 2012;18(3):305-313.
16. He J, Zhu Z. The relation of South China sea monsoon onset with the subsequent rainfall over the subtropical East Asia. Int. J. Climato. 2015;35(15):4547-4556.
17. Marteau, Phillipon, Fontaine, Moron. Approche multi-scalaire du démarrage de la saison des pluies au Sahel central et occidental: Cohérence spatiale et prévisibilité (Multiscalar approach of the onset of rainy season in central and western Sahel: Spatial coherence and predictability). Bulletin de l'Association de géographes français. 2010;87(2):207-220.
18. Balme M, Galle S, Lebel T. Démarrage de la saison des pluies au Sahel: Variabilité aux échelles hydrologique et agronomique, analysée à partir des données EPSAT-Niger. Sécheresse; 2004b.
19. Sijikumar S, Roucou P, Fontaine B. Monsoon onset over Sudan-Sahel: Simulation by the regional scale model MM5. Geophys Res Lett. 2006;33: L03814.
DOI: 10.1029/2005GL024819
20. Diallo I, Bain CL, Gaye AT, Moufouma-Okia W, Niang C, Dieng MDB, Graham R. Simulation of the West African monsoon onset using the HadGEM3-RA regional climate model. Clim Dyn. 2014;43:575–594.
DOI: 10.1007/s00382-014-2219-0b
21. Uppala SM, Dee D, Kobayashi S, Berrisford P, Simmons A. Towards a climate data assimilation system: Status update of ERA-Interim. ECMWF New Sletter. 2008;115:12-8.
22. Nikulin G, Jones C, Giorgi F, Asrar G, Büchner M, Cerezo-Mota R, et al. Precipitation climatology in an ensemble of CORDEX-Africa regional climate simulations. Journal of Climate. 2012;25: 6057-78.
DOI: 10.1175/JCLI-D-11-00375.1
23. Kim J, Waliser DE, Mattmann CA, et al. Evaluation of the CORDEX-Africa multi-RCM hindcast: Systematic model errors. Climate Dynamics. 2014;42(5-6):1189–1202.

24. Gbobaniyi E, Sarr A, Sylla MB, Diallo I, Lennard C, Dosio A, et al. Climatology, annual cycle and interannual variability of precipitation and temperature in CORDEX simulations over West Africa. International Journal of Climatology. 2014;34(7):2241–2257.
DOI: 10. 1002/joc.3834
25. Giorgi F, Jones C, Asrar G. Addressing climate information needs at the regional level: The CORDEX framework. WMO Bulletin. 2009;58175-183.
26. Paeth H, Capo-Chichi A, Endlicher W. Climate change and food security in tropical West Africa. Erdkunde. 2008;62: 101-15.
27. Adler RF, Huffman GJ, Chang A, et al. The version-2 global precipitation climatology project (GPCP) monthly precipitation analysis (1979-present). Journal of Hydrometeorology. 2003;4(6):1147–1167.
28. Huffman GJ, Adler RF, Bolvin DT, Gu G. Improving the global precipitation record: GPCP version 2.1. Geophys Res Lett. 2009;36(17):L17-808.
29. Baldauf M, Seifert A, Förstner J, Majewski D, Raschendorfer M, Reinhardt T. Operational convective-scale numerical weather prediction with the COSMO model: Description and sensitivities. Mon. Wea. Rev. 2011;139:3887–3905.
DOI: 10.1175/MWR-D-10-05013.1
30. van Meijgaard E, van Ulft LH, van de Berg WJ, Bosveld FC, van den Hurk BJJM, Lenderink G, Siebesma AP. The KNMI regional atmospheric climate model, version 2.1, KNMI Tech. Rep. 302, De Bilt, Netherlands; 2008.
31. Samuelsson P, Jones CG, Willén U, Ullerstig A, Gollvik S, Hansson U, et al. The ross by centre regional climate model RCA3: Model description and performance. Tellus A. 2010;63:4-23.
32. Scinocca JF, McFarlane NA, Lazare M, Li J. The CCCma Third generation AGCM and its extension into the middle atmosphere. Atmospheric Chemistry and Physics. 2008;8:7055-7074.
33. Christensen JH, Carter TR, Rummukainen M, Amanatidis G. Evaluating the performance and utility of regional climate models: The PRUDENCE project. Climatic Change. 2000;81:1-6.
34. Dee DP, Uppala SM, Simmons AJ, et al. The era-interim reanalysis: Configuration and performance of the data assimilation system. Q.J.R. Meteorol. Soc. 2011; 137(656):553-597.
35. Camara M, Diédhiou A, Sow BA, Diallo MD, Diatta S, Mbaye I, Diallo I. Analyse de la pluie simulée par les modèles climatiques régionaux de CORDEX en Afrique de l'Ouest. Sécheresse. 2013; 24(1).
36. Klutse NAB, Sylla MB, Diallo I, Sarr A, Dosio A, Diedhiou A, et al. Daily characteristics of West African summer monsoon precipitation in CORDEX simulations. Theoretical and Applied Climatology; 2015.
DOI: 10.1007/s00704-014-1352-3
37. Sarr AB, Camara M, Diba I. Spatial distribution of CORDEX regional climate models biases over West Africa. International Journal of Geosciences. 2015;6:1018-1031.
DOI: 10.4236/ijg.2015.69081
38. Akinsanola AA, Ogunjobi KO, Gbode IE, Ajayi VO. Assessing the capabilities of three regional climate models over CORDEX Africa in simulating west African summer monsoon precipitation. Advances in Meteorology. 2015;13.
(Article ID 935431)
DOI: 10.1155/2015/935431
39. Yamada TJ, Kanae S, Oki T, Hirabayashi Y. The onset of the West African monsoon simulated in a high-resolution atmospheric general circulation model with reanalyzed soil moisture fields. Atmos Sci Lett. 2012; 13:103–107.
DOI: 10.1002/asl
40. Thorncroft CD, Hanh N, Zhang CD, Peyrille P. Annual cycle of the West African monsoon: Regional circulations and associated water vapor transport. Q J R Meteorol. Soc. 2011;137:129–147.
DOI: 10.1002/qj.728
41. Cook KH. Generation of the African easterly jet and its role in determining west African precipitation. J Climate. 1999;12: 1165–1184.
42. Thorncroft CD, Blackburn M. Maintenance of the African easterly Jet. Q J R Meteorol Soc. 1999;125:763–786.
43. Sylla MB, Gaye AT, Pal JS, Jenkins GS, Bi XQ. High resolution simulation of West Africa climate using regional climate model (RegCM3) with different lateral boundary conditions. Theor Appl Climatol; 2009.
DOI: 10.1007/s00704-009-0110-4
44. Grist JP, Nicholson SE. A study of the dynamic factors influencing the interannual

variability of rainfall in the West African Sahel. Journal of Climate. 2001;14:1337–1359.

45. Diaconescu EP, Scinocca PGJ, Laprise René. Evaluation of daily precipitation statistics and monsoon onset/retreat over western Sahel in multiple data sets. Clim Dyn. 2015;45:1325-1354.
DOI: 10.1007/s00382-014-2383-2

46. Sylla MB, Giorgi F, Coppola E, Mariotti L. Uncertainties in daily rainfall over Africa: Assessment of observation products and evaluation of a regional climate model simulation. International Journal of Climatology; 2013.
DOI: 10.1002/joc.3551

Peer-review history:
The peer review history for this paper can be accessed here:
http://www.sciencedomain.org/review-history/26201